Semi-Interpenetrating Novolac-Epoxy Thermoset Polymer Networks Derived from Plant Biomass

Mehul Barde[1,2] , Yusuf Celikbag[3], Brian Via[3], Sushil Adhikari[4] and Maria L. Auad[1,2]*

[1]*Center for Polymers and Advanced Composites, Auburn University, Auburn, 36849, AL, United States of America.*
[2]*Department of Chemical Engineering, Auburn University, Auburn, 36849, AL, United States of America.*
[3]*Forest Products Development Center, Auburn University, Auburn, 36849, AL, United States of America.*
[4]*Department of Biosystems Engineering, Auburn University, Auburn, 36849, AL, United States of America.*

ABSTRACT: Bio-based phenol-formaldehyde polymer (BioNovolac) was developed by reacting molar excess of bio-oil/phenol with formaldehyde in acidic medium. Glycidyl 3,5-diglycidoxybenzoate (GDGB), was prepared by direct glycidylation of α-resorcylic acid (RA), a naturally occurring phenolic monomer. GDGB was crosslinked in the presence of BioNovolac by anionic polymerization. Fourier transform infrared spectroscopy (FTIR) confirmed the formation of semi-interpenetrating polymer networks. The glass transition temperature and moduli of bio-based crosslinked systems were observed to increase with increasing GDGB content. Active chain density and mass retention measured by dynamic mechanical analysis (DMA) and Soxhlet extraction, respectively, indicated a high crosslink density of the cured networks. Scanning electron microscopy (SEM) images depicted the homogeneity of the bulk phase. The preparation of bio-based epoxy-novolac thermoset network resulted in reduced consumption of petroleum-based chemicals.

KEYWORDS: Fast pyrolysis, bio-oil, BioNovolac, semi-interpenetrating polymer networks

1 INTRODUCTION

Increased scientific attention to the use of biomass is due to an increased demand for alternate resources for energy and materials. In anticipation of an increasing gap between supply and demand of petroleum, the market has been inclined to perform more research on the better utilization of biomass. Biomass is advantageous because it is abundant, renewable and carbon-neutral. There are opportunities to modify the biomass components for the production of the fuels, chemicals and materials [1]. In order to reduce the complexity of the biomass and to make it more efficiently usable for fuels and chemicals, various thermochemical and bio-chemical conversion processes have been developed. Pyrolysis, a thermochemical conversion process carried out in the absence of oxygen and at high temperature (around ~500°C), is beneficial in terms of producing high yields of the liquid fraction, i.e. bio-oil [2]. When a high heating rate and short vapor residence time is used, the pyrolysis process is termed fast pyrolysis [2-4]. Bio-oil contains different classes of organic compounds such as sugars, phenolic oligomers and monomers, aldehydes, carboxylic acids, alcohols, ketones and furans [5] which can be utilized as monomers for polymer synthesis.

*Corresponding author: auad@auburn.edu

DOI: 10.32604/JRM.2018.00116

In particular, crosslinked thermosetting polymers offer versatility by providing a wide range of properties such as high chemical resistance, heat resistance, high tensile strength and modulus, high glass transition temperature etc. due to the crosslinked structure [6]. Traditionally, crosslinked structures are built by grafting polymeric chains by crosslinking agent to form a continuous network. In case of traditional phenol-formaldehyde systems, oligomeric phenol-formaldehyde resin is synthesized by reaction of phenol and formaldehyde. The oligomeric resin is further crosslinked either by heating or by reacting with crosslinking agents such as hexamethylenetetramine. Epoxy systems are another famous example of crosslinkable polymers in which oligomeric/prepolymeric epoxide is reacted with amine, anhydride hardeners to yield a crosslinked material. Depending on crosslinking conditions, the grafts joining polymer chains can arise from crosslinking agents (amine, anhydrides for epoxides; and hexamethylenetetramine for phenol-formaldehyde) or from the polymer itself (unreacted functional groups of the oligomeric phenol-formaldehyde resin). An interpenetrating polymer network (IPN) can be formed with two or more polymer networks of which at least one of the networks is crosslinked in the presence of the other either simultaneously or sequentially [7, 8]. In such cases, networks are not grafted to each other at all crosslinking sites; rather their chains are entangled at the molecular level. Similarly, a semi-interpenetrating polymer network (semi-IPN) is a result of one

polymer network crosslinked in the presence of a linear or branched, non-crosslinked polymer. IPNs offer benefits in terms of synergism of the properties of two individual polymer networks [9, 10].

Phenol-formaldehyde and epoxy have been very important thermosetting resins due to their high market share and diverse applications such as adhesives, coatings, industrial laminates, abrasive materials [11]. Phenol is the precursor of phenol-formaldehyde resins and it is derived from petroleum. Phenol can be replaced by naturally occurring compounds and thus, modified phenol-formaldehyde resins can be developed. An example of naturally occurring substituted phenol is cardanol which can be extracted from cashew nut shell liquid. Synthesis and characterization of cardanol-based phenolic resins were studied by several researchers [12-15]. Vanillin, another naturally occurring substituted phenol, was co-reacted with furfural and 4-methylacetophenone in acidic medium to yield a bio-based phenol-formaldehyde resin [16]. Varying types of lignin were reacted, without further modifications, with phenol and formaldehyde to produce lignin-phenol-formaldehyde novolac resins [17]. Lignin is a natural polymer found in plant biomass and forms hemicellulose-lignin modules which bind the cellulose microfibrils bundles, thereby providing strength to the plant cell walls [18]. It consists of polyphenolic, macromolecular, complex structure [19, 20]. Lignin can be broken down to oligophenolic molecular structures that can be re-polymerized to a more specific phenol-formaldehyde type skeleton. Bio-based phenolic foams were prepared by using hydrolysis lignin depolymerized by a low temperature and low pressure method [21]. Since pyrolysis and liquefaction can be often used to break down lignin along with cellulose and hemi-cellulose, mono-phenols or oligophenolic structures can be found in the liquid bio-oil. Phenol was partially replaced by phenolic-rich fraction of the bio-oil to synthesize resol-type phenol-formaldehyde resins [22]. In addition, resol resins were also attempted by modifying the bark autoclave extractives [23]. In another study, formate-assisted fast pyrolysis was used to obtain bio-oil which was reacted with formaldehyde in acidic medium for preparing novolac-type resins [24]. Effendi et al. have critically reviewed the phenolic resins produced by thermochemical conversion of plant biomass [25].

Epoxy resins are polymeric materials capable to serve many applications; and have competed with phenolic resins for a long period. Tremendous amount of research has been carried out on epoxy resins and their applications. There is a vast scope to design molecular structures of prepolymeric epoxides and curing agents; and the properties can be altered accordingly. Epoxy resins most commonly appear as diglycidyl ether of bisphenol-A (DGEBA) and its oligomers, all of which are synthesized from bisphenol-A (BPA) and epichlorohydrin [26, 27]. Bisphenol-A is not only a petroleum-derived compound but also can affect human health.[28] In an attempt to avoid the use of bisphenol-A, epoxy resins have been successfully derived from fatty acid triglycerides present in vegetable plant oil. Fatty acid chains of several oils such as soybean oil, linseed oil, tung oil, dehydrated castor oil contain unsaturation and can be derivatized to oxirane functionality [29, 30]. These resin structures are mainly composed of aliphatic chains due to the involvement of aliphatic acids. Absence of aromaticity can result in reduced mechanical performance [6]. Aromatic moieties from bio-based resources have been successfully introduced in epoxy resins by epoxidizing phenolic hydroxyl groups appearing in bark extractives [31,32], tannins [33], biomass pyrolysis oil [34] and hydrothermal liquefaction oil [35]. Our previous work focused on the synthesis and evaluation of thermoset networks of epoxy resin derived from 3,5-dihydroxybenzoic acid [36, 37]. With a more commonly accepted name, α-resorcylic acid, it is a monocylic aromatic monomer naturally occurring in red sandalwood, hill raspberry, chickpeas and peanuts [38]. In comparison with bisphenol-A that has two aromatic rings per molecule, the reduction of hydrophobic content per molecule due to the single aromatic ring may decrease the binding tendency of α-resorcylic acid to estrogen receptor [28]. Decreased interaction with the receptor and natural occurrence of α-resorcylic acid can potentially make it to be a replacement of bisphenol-A. The resulting epoxy resin, with three epoxide rings per molecule, offers the advantage of having a low epoxy equivalent weight (hence, a high epoxy content) and low viscosity [36, 37]. The present work is mainly focused on developing interpenetrating networks of bio-oil based novolac polymers and epoxy resins derived from α-resorcylic acid.

2 EXPERIMENTAL SECTION

2.1 Materials

Fast pyrolysis bio-oil derived from hardwood was obtained from Red Arrow, USA. Phenol (detached crystals, 99%), formalin solution (37% w/w), acetone, methanol, sodium hydroxide, (±)-epichlorohydrin (99%), 3,5-dihydroxybenzoic acid, chromium(III)acetyl acetonate, N-hydroxy-5-norbornene-2,3-dicarboximide (NHND), deuterated chloroform were purchased from VWR International. 2-Chloro-4,4,5,5-tetramethyl-1,3,2-dioxaphospholane (TMDP) was ordered from Sigma Aldrich. Oxalic acid, anhydrous, was supplied by

Spectrum Chemical Mfg. Corp. Benzyltriethylammonium chloride was obtained from TCI. 4-(Dimethylamino) pyridine (DMAP) (prilled, 99%) was ordered from Beantown Chemical.

2.2 Methods

2.2.1 Characterization of fast pyrolysis bio-oil

Fast pyrolysis bio-oil contained water and was removed by using rotary evaporator. After removal of water, the chemical composition of bio-oil was qualitatively analyzed by Gas Chromatography-Mass Spectroscopy (GC-MS) according to the procedure reported [39]. Around 0.5 g of bio-oil was diluted with 12 mL of methanol and mixed well. A split ratio of 20:1 was set for injecting 1 μL of diluted bio-oil into a DB-1701 column equipped to an Agilent 7890 GC/5975MS. The hydroxyl (OH) content of bio-oil was quantitatively measured by ^{31}P-NMR as per the procedure mentioned [40]. The stock solution was prepared by dissolving 40 mg of NHND and 40 mg of chromium(III)acetyl acetonate in the mixture of 6 mL pyridine and 4 mL deuterated chloroform. Approximately 20 mg of bio-oil was dissolved in 500 μL of stock solution. 150 μL of TMDP was added to the mixture to phosphitylate the hydroxyl groups in bio-oil. The sample was then transferred to the NMR tube and the spectrum was acquired with a Bruker Advance II 250 MHz spectrometer using inverse gated decoupling pulse sequence, 90 degree pulse angle, 25 s pulse delay and 128 scans.

2.2.2 Synthesis of novolac and bionovolac resins

Novolac resin (phenol-formaldehyde resin synthesized with molar excess of phenol over formaldehyde in acidic medium) was synthesized as per the procedure described in the literature [41]. The molar ratio of phenol to formaldehyde was kept constant at 1:0.8 for all resin formulations. Oxalic acid (0.0522 per mol of phenol) was added to the reaction flask and the temperature was raised to 90°C. The calculated amount of formaldehyde aqueous solution (formalin, 37%) was added dropwise to the constantly agitated reaction mixture and the reaction was continued at 90°C for next three hours. BioNovolac resins were synthesized by the same procedure, replacing phenol with bio-oil in varying proportions. A specific amount of phenol was replaced by bio-oil on weight basis (10%, 50%), and the oxalic acid was added to the physical blend of fast pyrolysis bio-oil and phenol. The progress of reaction was monitored by Fourier Transform Infrared (FTIR) spectroscopy. The synthesis routes and the structures of Novolac and BioNovolac resins are shown in Figure 1.

2.2.3 Synthesis of glycidyl 3,5-diglycidoxybenzoate (GDGB)

In order to carry out glycidylation of α-resorcylic acid, the procedure was used as per the literature [33, 42]. Epichlorohydrin (4 M eq/OH) was added to RA and the temperature was raised to 100°C. Benzyltriethylammonium chloride (0.012 M eq/OH) was added as the phase transfer catalyst. The reaction was carried out for 1 h to produce chlorohydrin intermediate and the reaction mixture was cooled down to 30°C. An aqueous solution of sodium hydroxide (2 M eq/OH) was added along with the same previous amount of benzyltriethylammonium chloride and the reaction was continued for 90 min. The organic layer was separated and washed with water to remove the salt. The product was further purified by removing unreacted epichlorohydrin at 90°C under reduced pressure by rotary evaporation. A stepwise synthesis of GDGB is depicted in Figure 2.

2.2.4 Determination of epoxy equivalent weight (EEW)

The epoxy equivalent weight was measured by the hydrogen bromide-glacial acetic acid solution method. Around 0.3-0.4 g of sample was taken in a 50 mL Erlenmeyer flask and 10 mL acetone was added to it. The contents of the flask were stirred well so as to dissolve GDGB sample in acetone. Just before the titration, a drop of crystal violet indicator solution (1 g/L, in glacial acetic acid) was added and the contents were titrated with 0.1 N HBr-glacial acetic acid solution until the end point "blue-green color" persisted for 30 s. The epoxy equivalent weight (EEW) was calculated as per the following formula:

$$\text{EEW} = \frac{1000 \times (\text{wt.of sample})}{\text{N} \times \text{V}} \quad (1)$$

where, N=Normality of HBr-glacial acetic acid solution
V=Volume of HBr-glacial acetic acid solution required to titrate the sample.

2.2.5 Crosslinking of thermoset polymer networks

GDGB was crosslinked in the physical presence of BioNovolac polymers. Varying amounts of 10% BioNovolac and 50% BioNovolac were separately blended with GDGB before curing. All thermoset systems were prepared by crosslinking with 0.08 mol of 4-(dimethylamino) pyridine (DMAP) per epoxide. Anionic addition polymerization of epoxides by DMAP is reported elsewhere [43]. The initiator quantities required are considerably less as compared to that of amine hardeners traditionally used for curing epoxides and help to reduce the overall consumption of petroleum-derived compounds. The curing procedure consisted of heating the samples in aluminum molds in a conventional oven at 60°C for 2 h followed by 80°C, 90°C, 100°C, 120°C, 140°C for 1 h each and finally at 165°C for 15 min.

2.2.6 FTIR analysis

Novolac, BioNovolac and GDGB were analyzed by Fourier transform infrared spectroscopy (FTIR) which was performed with attenuated total reflection (ATR) method using Thermo Scientific Nicolet 6700 FT-IR spectrophotometer and OMNIC 7.3 software. The spectra were collected in the wavenumber range 400 cm^{-1} to 4000 cm^{-1} at a resolution of 4 cm^{-1} and 40 scans. Cured thermosets were also analyzed by FTIR to confirm several phenomena such as ring opening of epoxides, grafting of polymeric chains and semi-IPN formation.

2.2.7 Evaluation of thermo-mechanical performance

Dynamic mechanical analysis is generally used to observe the viscoelastic region of the polymeric system. A cyclical strain is applied while increasing the temperature and the dynamic mechanical moduli are measured. The storage modulus is indicative of the energy stored elastically while the loss modulus is the characteristic energy lost via heat [44]. The tangent of the phase angle between cyclic strain and cyclic stress, or in other terms, the ratio of loss modulus to the storage modulus is termed as tanδ, the maximum of which appears generally at the glass transition temperature of the polymeric system. Therefore, this technique can be used to measure the glass transition temperature of the crosslinked systems. In the current study, a three point bending geometry was used with a TA Instruments RSAIII Dynamic Mechanical Analyzer, on the samples with approximate dimensions of 25×10×3 mm. A constant strain of 0.1% and cyclic frequency of 1 Hz was applied while increasing the temperature from 25°C to 200°C at 10°C/min. The storage modulus and tanδ were plotted against temperature and the glass transition temperature was measured at the maximum tanδ. The active chains density was calculated by the following formula

$$n = \frac{E'}{3RT} \quad (2)$$

where E' is storage modulus (Pa) at the temperature T T is (glass transition temperature+50) expressed in Kelvin, and R is the universal gas constant, 8.314 $Jmol^{-1}K^{-1}$. Differential scanning calorimetry was used to observe the glass transition temperature of the crosslinked polymer networks. The temperature was increased from 20°C to 200°C by the heating rate 10 °C/min, reduced from 200°C to 20°C by the cooling rate 20°C/min and was again increased to 200°C by the heating rate 10 °C/min.

For all crosslinked thermoset systems, Soxhlet extraction was carried out with a refluxing action of 200 mL dichloromethane for 24 h. After extraction, the residual solids were dried and weighed. Then mass retained was calculated by the following equation:

$$\text{Mass retained (\%)} = \frac{\text{Weight of dried solids after extraction}}{\text{Initial weight of solids}} \times 100 \quad (3)$$

Crosslinked systems of GDGB and 50% BioNovolac were analyzed under scanning electron microscope. The samples were immersed in liquid nitrogen and then cut to observe the cross-sections. All samples were sputter-coated with gold before SEM analysis.

3 RESULTS AND DISCUSSION

3.1 Characterization of Fast Pyrolysis Bio-oil

The peaks detected during GC-MS characterization of bio-oil, and corresponding compounds were identified using NIST (National Institute of Standards and Technology) mass spectral library and are depicted in Figure 3.

^{31}P-NMR characterization was successfully carried out to measure the total hydroxyl content as 5.80 mmol OH/g. The details of specific groups are shown in Table 1 and Figure 4. With the help of GC-MS and ^{31}P-NMR, monocylic phenolic compounds and phenolic hydroxyl groups were observed which led to a confirmation of presence of substituted phenols that might have formed after depolymerization of lignin during pyrolysis. Aliphatic alcohols, aldehydes, ketones, carboxylic acids and levoglucosan were also identified using GC-MS. Further, ^{31}P-NMR showed the presence of aliphatic hydroxyl and acidic hydroxyl groups, indicating that compounds other than substituted aromatics were present too due to the decomposition of cellulose and hemicelluloses during pyrolysis.

3.2 Characterization of the Bionovolac Resins

Figure 5 shows the FTIR spectra of BioNovolac and Novolac resins. The same peaks with varying intensities were observed in all the spectra, which confirmed that the synthesis of BioNovolac resin followed a similar reaction pathway than the novolac resin. The decreasing intensity of the peaks corresponding to the bonds C=C (ar), C-O (ph) and =C-H (oop), with increasing bio-oil content is attributable to the reduction in total phenolic content of bio-oil/phenol blend. The bio-oil is not only comprised of substituted phenols but also contains many other organic compounds observed in GC-MS results. (Refer Figure 3). Formation of phenol-formaldehyde network is carried out by the selective reaction of formaldehyde at ortho and para sites of phenol and substituted phenols.

Table 1 Hydroxyl content determined by ^{31}P-NMR technique.

Hydroxyl Type			**Range (ppm)**	**Hydroxyl Content (mmol/g)**	
Aliphatic OH			150.00-145.50	3.58	3.58
Phenolic OH	C-5 substituted condensed phenolic OH	β-5	144.70-142.80	0.38	1.71
		4-O-5	142.80-141.70	0.33	
		5-5	141.70-140.20	0.26	
	Guaiacyl phenolic OH		140.20-139.00	0.31	
	Catechol type OH		139.00-138.20	0.33	
	p-hydroxy-phenyl OH		138.20-137.30	0.10	
Acidic OH			136.60-133.60	0.51	0.51
Total					5.80

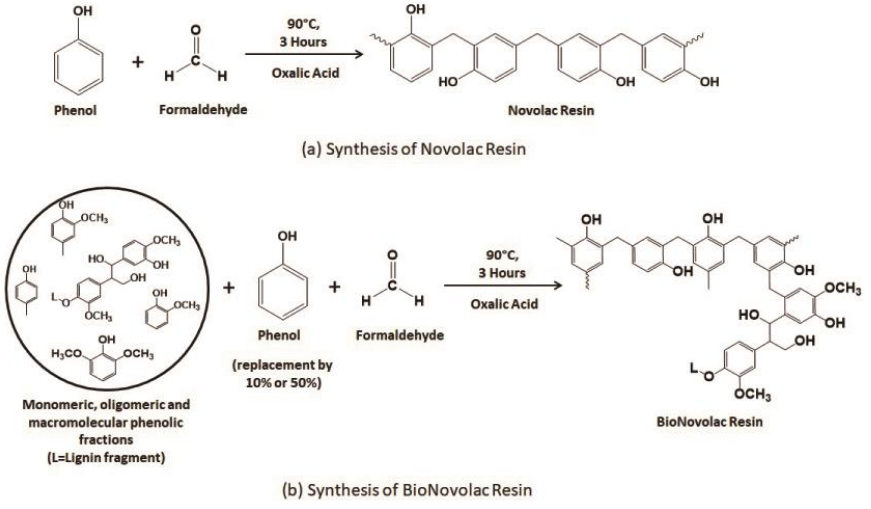

Figure 1 (a) Synthesis of novolac resin, (b) Synthesis of BioNovolac resin.

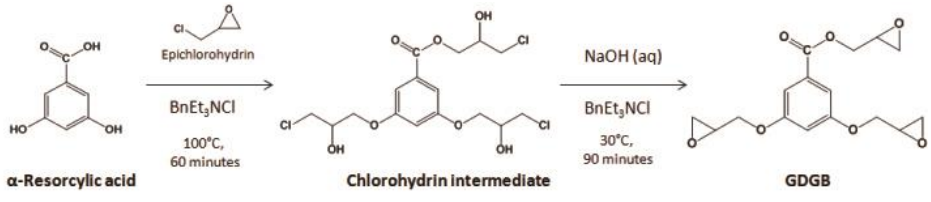

Figure 2 Glycidylation of α-resorcylic acid.

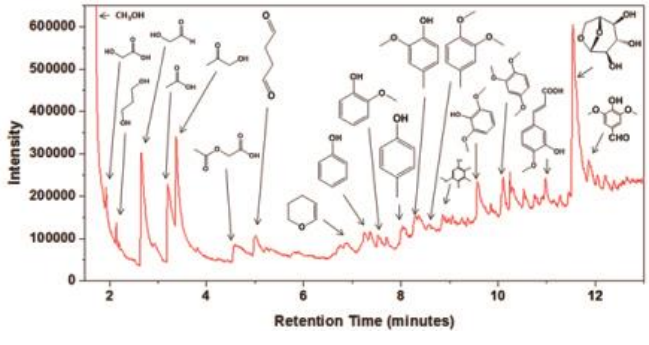

Figure 3 Compositional Analysis of Bio-oil by GC-MS.

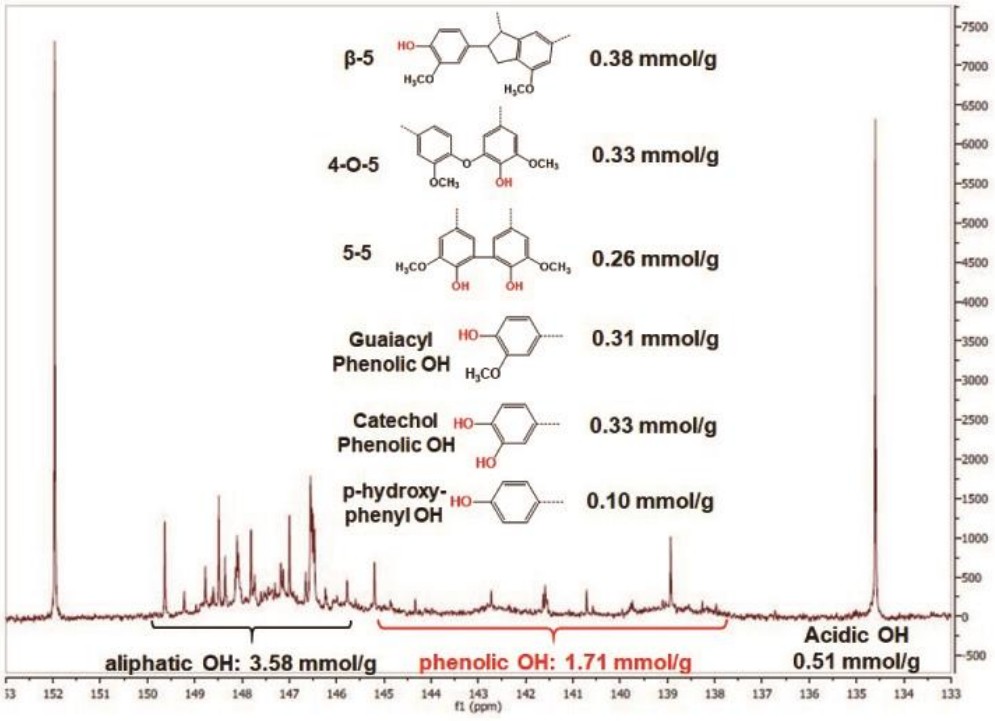

Figure 4 ^{31}P-NMR analysis of Bio-oil.

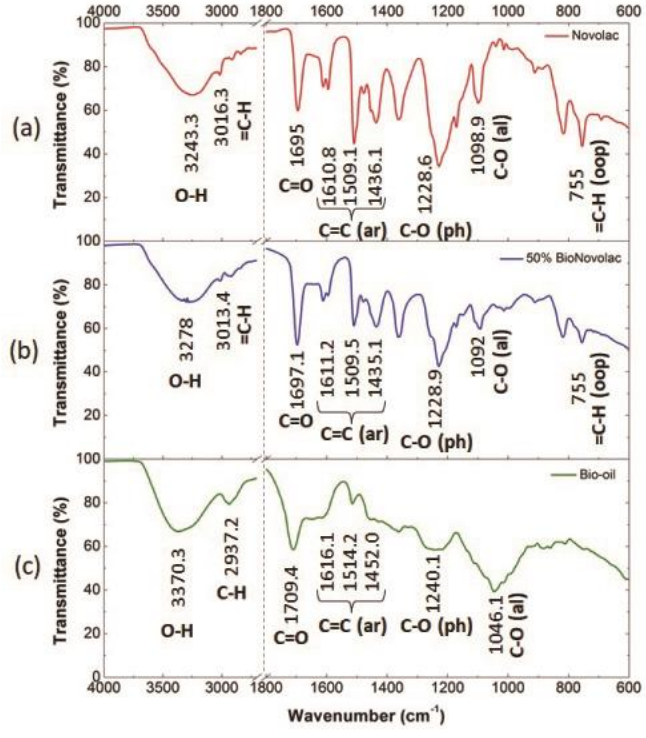

Figure 5 FTIR spectra of (a) novolac (b) 50% BioNovolac and (c) bio-oil. Notes: ar-aromatic, ph-phenolic, oop-out of plane bending, al-aliphatic.

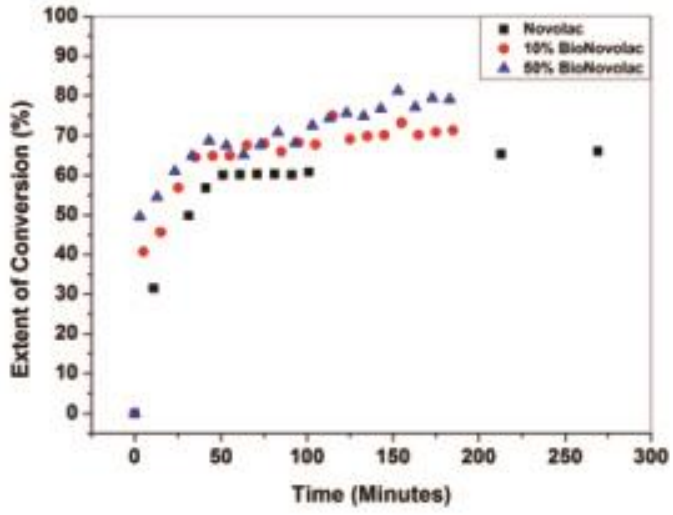

Figure 6 BioNovolac Extent of Conversion (Refer Equation (4)).

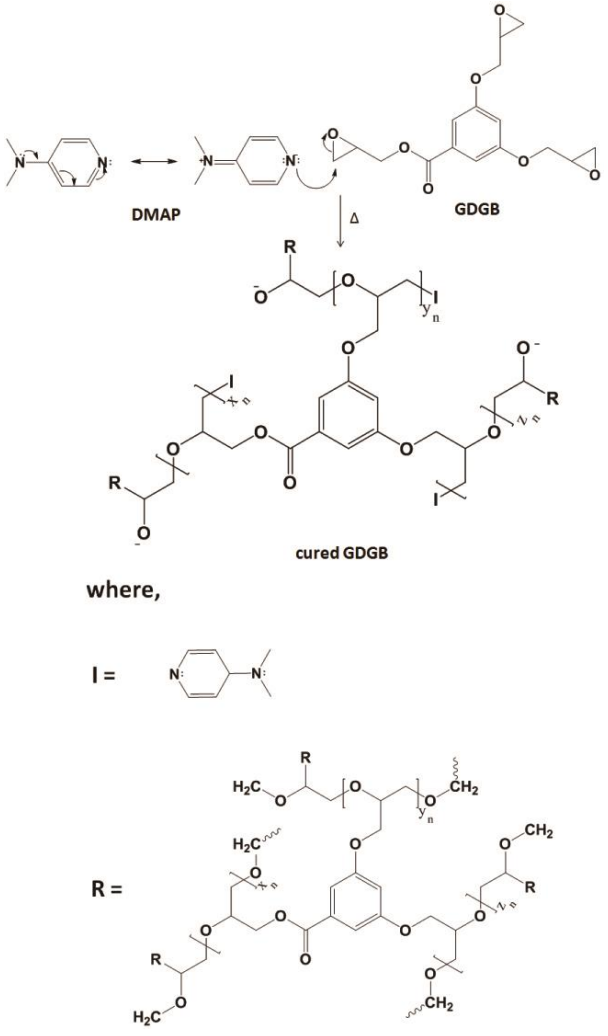

Figure 7 Crosslinking of GDGB by DMAP.

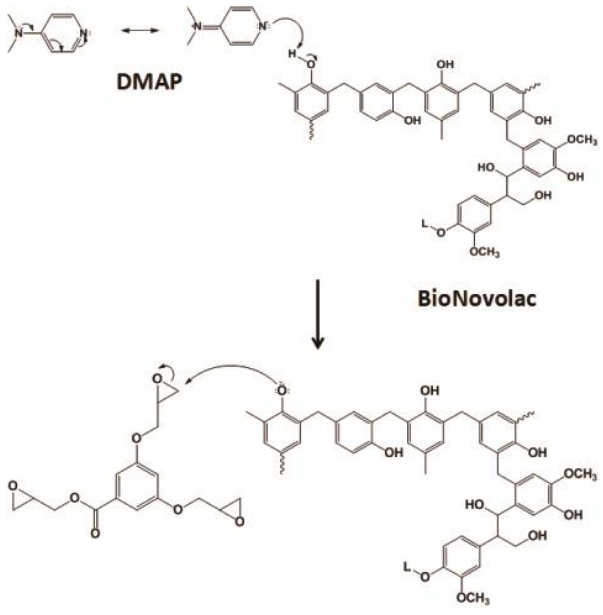

Figure 8 Grafting of BioNovolac and GDGB Networks.

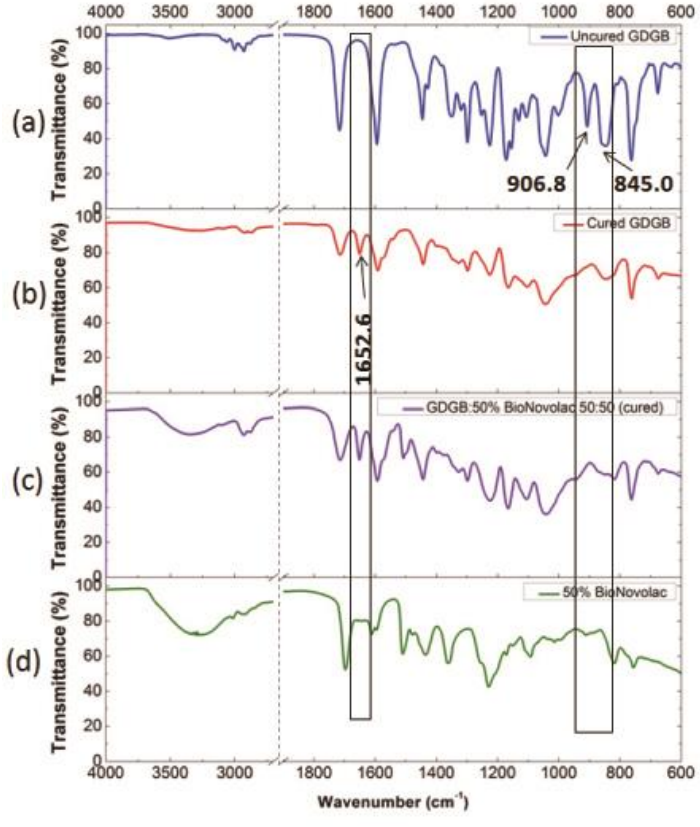

Figure 9 FTIR spectra of (a) uncured GDGB (b) cured GDGB (c) cured GDGB: 50% BioNovolac 50:50 and (d) 50% BioNovolac.

The progress of reaction of Novolac, 10% BioNovolac and 50% BioNovolac was observed using a peak at 755 cm^{-1} that reflects the aromatic C-H out of plane vibration band. The intensity of the peak reduced with time due to the formation of C-C bond at ortho/para positions. The extent of conversion of phenolic

monomers, x_t, is calculated by the formula reported in the literature [45].

$$x_t = \left(1 - \frac{\text{peak height at time t}}{\text{initial peak height}}\right) \times 100 \qquad (4)$$

Figure 6 contains the plot of the extent of conversion of phenolic monomers with time. The extent of conversion of phenolic monomers in all three reactions had a similar trend.

3.3 Characterization of Glycidyl 3,5-Diglycidoxybenzoate (GDGB)

FTIR analysis of GDGB has been carried out extensively and led to the detection of several important peaks. Figure 9(a) displays FTIR spectra of GDGB. A broad peak at 3188 cm^{-1} present in α-resorcylic acid, corresponding to O-H stretching vibrations disappeared in the spectrum of GDGB due to the conversion of one carboxyl and two hydroxyl groups into glycidyl functionality. Epoxide ring formation was confirmed by the epoxide ring deformation bands at 906 cm^{-1} (asymmetric) and 845 cm^{-1} (symmetric). Two bands that appeared due to C-O-C stretch were also observed at 1225 cm^{-1} (asymmetric) and 1043 cm^{-1} (symmetric). GDGB showed peaks responsible for C=C bonds in aromatic ring and C=O bond. The EEW for GDGB was experimentally found to be 106.83±3.02 g/eq which was comparable to the value reported earlier by Sibaja et al. [36].

The epoxy ring can be opened via nucleophilic attack by electron-rich nitrogen atom of DMAP as shown in Figure 7. Opening of the ring is followed by formation of an alkoxide anion, which attacks another epoxy ring, thereby creating a new alkoxide ion. In addition, the successive epoxy monomers leads to a chain reaction-anionic polymerization of epoxides; in the case of GDGB that has three epoxy rings, a three dimensional network is formed by this anionic polymerization. Figure 7 depicts the structure of cured GDGB network in which R is itself a macromolecular repeating unit and "I" belongs to the DMAP initiator

When BioNovolac is present along with GDGB, additional reaction can occur in which the DMAP initiator abstracts phenolic proton resulting in the formation of phenoxide anion which can open the epoxy rings (Refer Figure 8). The BioNovolac chains can be grafted to GDGB network. These reactions were observed with FTIR and are discussed in the next section.

In the cured GDGB-50%BioNovolac (50:50), opening of epoxy rings was confirmed by the disappearance of the epoxide ring deformation bands at 906 cm^{-1} (asymmetric) and 845 cm^{-1} (symmetric) as shown in Figure 9. It also depicts a peak corresponding to 1652 cm^{-1} due to overlap of vinylidene groups formed by chain transfer and iminium group resulted from DMAP. Figure 10 explains a general mechanism of intramolecular chain transfer. During chain transfer reactions, an initiator fragment can be detached to form an anion which can lead to further ring opening and a vinylidene group can be formed on the dead chain.

FTIR was used to observe the effect of DMAP on curing BioNovolac. Spectra of uncured BioNovolac were compared to the spectra of heated BioNovolac with and without addition of DMAP. In Figure 11, the peak near 1647.7 cm^{-1} can be attributed to formation of iminium ion discussed in previous section, while the peak corresponding to 1562.4 cm^{-1} is due to amine N-H of DMAP. The peak observed at 1362.7 cm^{-1} was contributed by in-plane bending of phenolic C-O-H groups and disappeared only in case of BioNovolac+DMAP combination since phenolic protons were abstracted by excess DMAP.

However, in presence of GDGB, all phenolic hydroxyl are generally not converted to phenoxide anions due to competing reaction of initiator and epoxy. Such a combination of competing reactions leads to the formation of a semi-interpenetrating polymer network in which BioNovolac polymer chains are grafted only at several points to the densely cured GDGB network.

3.4 Evaluation of Thermo-Mechanical Performance

With increasing amount of GDGB, storage moduli and glass transition temperatures of the cured systems enhanced. GDGB content was increased from 0 to 100 wt% by an interval of 25 wt%. It was observed that the GDGB-10% BioNovolac samples with 10% BioNovolac content more than 50% by weight, were brittle enough to be unable to be tested with DMA. Similar brittleness was observed for GDGB-50%BioNovolac samples with 50% BioNovolac content more than 75% by weight. The glass transition temperatures measured by DSC showed an increase with increasing the GDGB content, and followed the same trend indicated by the glass transition temperatures measured by DMA. Fox equation (Refer Equation (5)) was used to predict the glass transition temperature profile and the experimental values were found to be in agreement with the predicted values. (Refer Figure 12(a) and Figure 12(b).

$$\frac{1}{T_{g,\ \text{predicted}}} = \frac{f_{GDGB}}{T_{g,\ GDGB}} + \frac{f_{BioNovolac}}{T_{g,\ BioNovolac}} \qquad (5)$$

where, f=weight fraction

T_g=glass transition temperature, K

Table 2 lists the values of glass transition temperature, storage modulus, active chains density and mass retained for the thermoset networks. The glass

transition temperature was measured by DMA (tanδ peak) as well as DSC (change in the slope of heat flow). It was observed that the active chains density decreased with decreasing GDGB content. Increasing bio-content of BioNovolac improved active chain density. This is probably due to the impact of the polymeric structure of lignin fragments present in the bio-oil on the BioNovolac properties. The mass retained was more than 75% for all the systems with most being in the range 88-99%, after 24 h of extraction with dichloromethane.

Table 2 Thermo-mechanical properties of thermosets

System	**Tg (°C), DMA**	**Tg (°C),DSC**	**E'(GPa) at room temperature**	**Active Chains Density, n (mol/m³)**	**Mass (%) Retained**
GDGB	161	161	1.78	13721	93.81
GDGB : 10% BioNovolac					
75:25	125	128	1.88	2759	88.85
50:50	109	106	1.15	1119	92.66
25:75	N/A	94	N/A	N/A	79.38
10% BioNovolac	N/A	58	N/A	N/A	80.18
GDGB : 50% BioNovolac					
75:25	139	138	2.59	6355	98.69
50:50	104	106	2.65	1793	97.91
25:75	100	92	0.30	31	95.85
50% BioNovolac	N/A	70	N/A	N/A	78.37

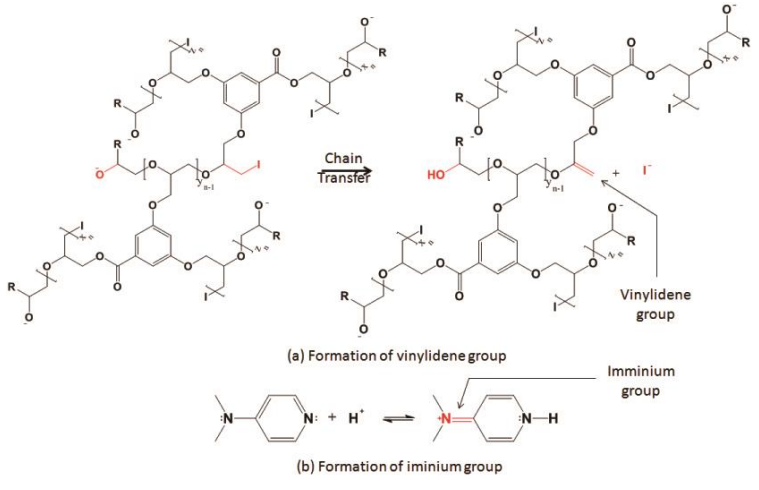

Figure 10 Species responsible for IR peak at 1652 cm^{-1} in cured networks.

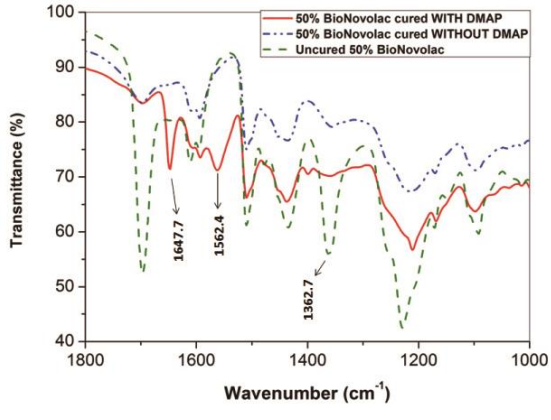

Figure 11 Curing of 50%BioNovolac, with and without DMAP.

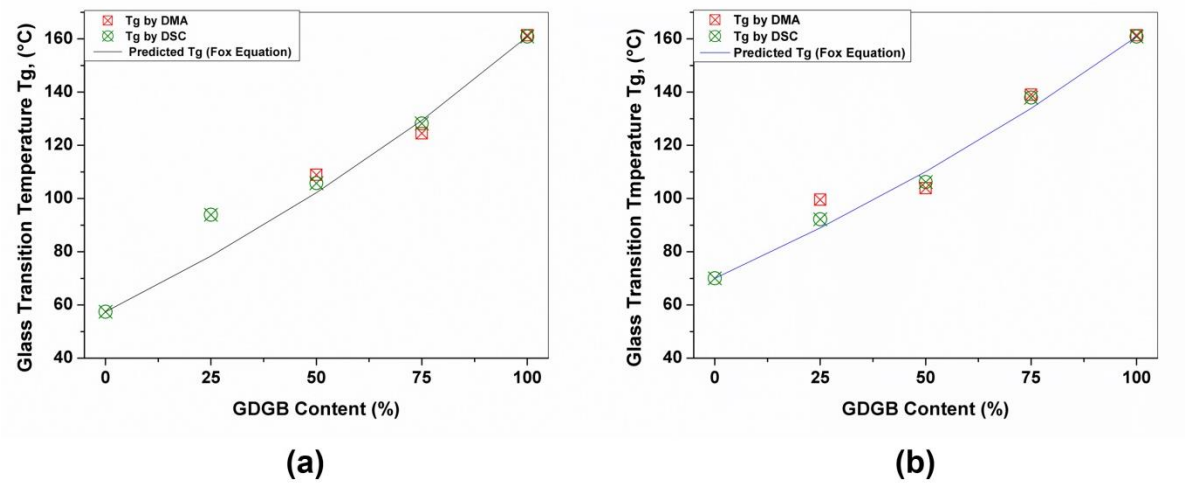

Figure 12 Glass transition temperature of semi-IPNs with (a) 10% BioNovolac (b) 50% BioNovolac.

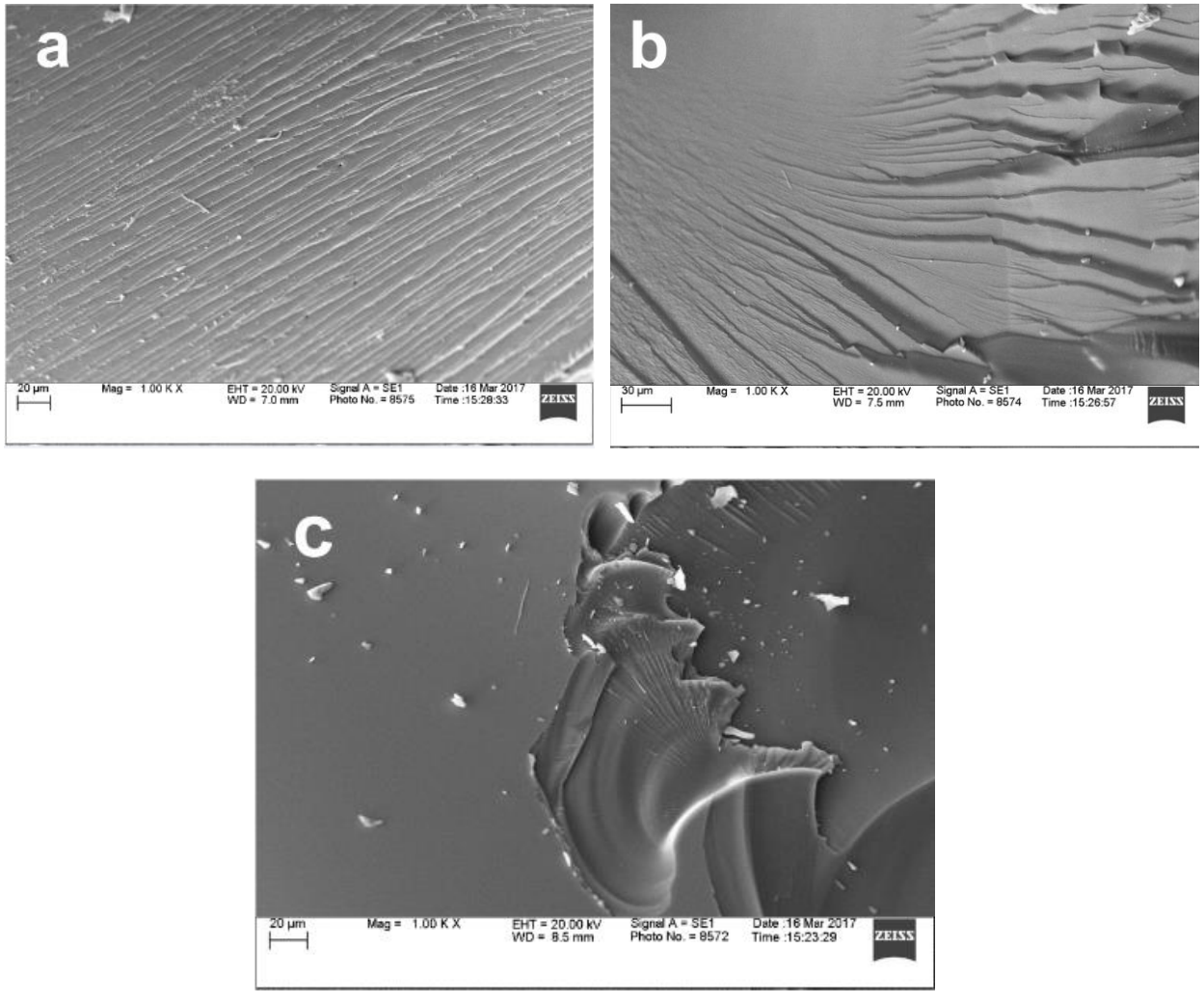

Figure 13 SEM Photographs (a) cured GDGB (b) cured GDGB: 50% BioNovolac (50:50) (c) uncured 50% BioNovolac.

Figures 13(a), 13(b) and 13(c) include the comparison of morphology of three systems (GDGB-50% BioNovolac) with varying ratios. The samples show similar fracture lines at the cross-sections, with negligible phase separation observed. Maximum brittle lines were observed in case of cured GDGB. The brittle lines decreased with increasing amount of 50% BioNovolac. In other words, brittleness reduced with increasing 50% BioNovolac content due to reduction in the active chains density. This phenomenon is in agreement with the observed thermo-mechanical results too.

4 CONCLUSIONS

It can be concluded that the compounds present in the fast pyrolysis bio-oil can be selectively polymerized to phenol-formaldehyde polymers-BioNovolac resins. BioNovolac can be blended homogeneously with GDGB, a resin that is not derived from bio-oil, and hence proves the compatibility of complex structured, high molecular weight BioNovolac with a simple, low molecular weight GDGB. GDGB can be densely crosslinked via anionic polymerization route; however, BioNovolac polymers cannot be homo-linked by DMAP. Nevertheless, the graft points between BioNovolac and GDGB networks prove that it is a semi-interpenetrating polymer network in which long chains of BioNovolac are interpenetrated in the presence of GDGB polymer network. The crosslinked networks show high thermo-mechanical performance and high glass transition temperatures. It is also important to note that the utilization of fast pyrolysis bio-oil, α-resorcylic acid and anionic polymerization initiator reduced the amount of petroleum-derived compounds. Since phenol was partially replaced in the synthesis of BioNovolac and bisphenol-A was not used at all, the thermoset networks are expected to have reduced toxicity concerns.

ACKNOWLEDGEMENTS

The authors would like to acknowledge US Department of Agriculture-National Institute of Food and Agriculture (USDA-NIFA-2015-67021-22842) and NSF-CREST Center of Excellence in Nano-Bio Materials derived from biorenewable and waste resources for funding this study. Additionally, this work was supported by the Agriculture and Food Research Initiative-"Hydrophobic Bio-Oil-Epoxy Binders for Wood Composites" (Project Award Number 2017-67021-26134).

REFERENCES

1. A.J. Ragauskas, C.K. Williams, B.H. Davison, G. Britovsek, J. Cairney, C.A. Eckert, W.J. Frederick, J.P. Hallett, D.J. Leak, C.L. Liotta, J.R. Mielenz, R. Murphy, R. Templer and T. Tschaplinski, The path forward for biofuels and biomaterials. *Science* **311**, 484 (2006).
2. A.V. Bridgwater, D. Meier and D. Radlein, An overview of fast pyrolysis of biomass. *Organic Geochemistry* **30**, 1479 (1999).
3. D. Mohan, C.U. Pittman, P.H. Steele, Pyrolysis of wood/biomass for bio-oil: A critical review. *Energy Fuels* **20**, 848 (2006).
4. A.V. Bridgwater, Review of fast pyrolysis of biomass and product upgrading. *Biomass Bioenergy* **38**, 68 (2012).
5. M. Stas, D. Kubicka, J. Chudoba and M. Pospisil, Overview of analytical methods used for chemical characterization of pyrolysis bio-oil. *Energy Fuels* **28**, 385 (2014).
6. J.M. Raquez, M. Deleglise, M.F. Lacrampe and P. Krawczak, Thermosetting (bio)materials derived from renewable resources: A critical review. *Progress in Polymer Science* **35**, 487 (2010).
7. L. Sperling, H. and V. Mishra, The current status of interpenetrating polvrner networks. *Polymers for Advanced Technologies***7**, 197 (1996).
8. N. Gupta and A.K. Srivastava, Interpenetrating polymer networks-A review on synthesis and properties. *Polymer International* **35**, 109 (1994).
9. L. Maleki, U. Edlund and A.C. Albertsson, Synthesis of full interpenetrating hemicellulose hydrogel networks. *Carbohydrate Polymers* **170**, 254 (2017).
10. R. Ballestero, B.M. Sundaram, H.V. Tippur and M.L. Auad, Sequential graft-interpenetrating polymer networks based on polyurethane and acrylic/ester copolymers. *Express Polymer Letters* **10**, 204 (2016).
11. A. Knop and L.A. Pilato. *Phenolic Resins: Chemistry, Applications and Performance,* Springer-Verlag Berlin Heidelberg, New York and Tokyo, *1-307* (1985).
12. A. Devi and D. Srivastava, Cardanol-based novolac-type phenolic resins I: A kinetic approach. *Journal of Applied Polymer Science* **102**, 2730 (2006).
13. R. Yadav and D. Srivastava, Kinetics of the acid-catalyzed cardanol-formaldehyde reactions. *Materials Chemistry and Physics* **106**, 74 (2007).
14. N.L. Huong, N.H. Nieu, T.T.M. Tan, U.J. Griesser, Cardanol-phenol-formaldehyde resins: Thermal analysis and characterization. *Angewandte Makromolekulare Chemie* **243**, 77 (1996).
15. R. da Silva Santos, A.A. de Souza, M.A. De Paoli and C.M.L. de Souza, Cardanol–formaldehyde thermoset composites reinforced with buriti fibers: Preparation and characterization. *Composites Part A: Applied Science and Manufacturing* **41**, 1123 (2010).
16. N.P.S. Chauhan, Facile synthesis of environmental friendly halogen-free microporous terpolymer from renewable source with enhanced physical properties. *Des. Monomers Polym* **15**, 587 (2012).
17. A. Tejado, G. Kortaberria, C. Pena, J. Labidi, J.M. Echeverria, I. Mondragon, Lignins for phenol replacement in novolac-type phenolic formulations, part I: Lignophenolic resins

synthesis and characterization. *J. Appl. Polym. Sci.* **106**, 2313 (2007).
18. N. Terashima, K. Kitano, M. Kojima, M. Yoshida, H. Yamamoto and U. Westermark, Nanostructural assembly of cellulose, hemicellulose, and lignin in the middle layer of secondary wall of ginkgo tracheid. *Journal of Wood Science* **55**, 409 (2009).
19. S. Sen, S. Patil, D.S. Argyropoulos, Thermal properties of lignin in copolymers, blends, and composites: A review. *Green Chemistry* **17**, 4862 (2015).
20. A. Gandini, T.M. Lacerda, From monomers to polymers from renewable resources: Recent advances. *Progress in Polymer Science* **48**, 1 (2015).
21. B. Li, Y. Wang, N. Mahmood, Z. Yuan, J. Schmidt and C. Xu, Preparation of bio-based phenol formaldehyde foams using depolymerized hydrolysis lignin. *Industrial Crops and Products* **97**, 409 (2017).
22. S.S. Kelley, X.M. Wang, M.D. Myers, D.K. Johnson and J.W. Scahill, Use of biomass pyrolysis oils for preparation of modified phenol formaldehyde resins, in Developments in *Thermochemical Biomass Conversion*, A.V. Bridgwater, D.G.B. Boocock (Eds.), Chapman & Hall, London, 557-574 (1997).
23. Y. Zhao, N. Yan, M. Feng, Synthesis and characterization of bio-based phenol-formaldehyde resol resins from bark autoclave extractives. *Forest Products Society* **66**, 18 (2016).
24. A.E. Vithanage, E. Chowdhury, L.D. Alejo, P.C. Pomeroy, W.J. DeSisto, B.G. Frederick and W.M. Gramlich, Renewably sourced phenolic resins from lignin bio-oil. *Journal of Applied Polymer Science* **134**, 10 (2017).
25. A. Effendi, H. Gerhauser and A.V. Bridgwater, Production of renewable phenolic resins by thermochemical conversion of biomass: A review. *Renewable and Sustainable Energy Reviews* **12**, 2092 (2008).
26. B. Ellis, Introduction to the chemistry, synthesis, manufacture and characterization of epoxy resins, in *Chemistry and Technology of Epoxy Resins,* B. Ellis (Ed.), Chapman & Hall, London, 1-35 (1993).
27. W. Brostow, S.H. Goodman and J. Wahrm und, Epoxies, in *Handbook of Thermoset Plastics,* H. Dodiuk, S. H. Goodman (Eds.), Elsevier, San Diego, CA, 191-252 (2014).
28. F.F. Ng, G. Couture, C. Philippe, B. Boutevin and S. Caillol, Bio-based aromatic epoxy monomers for thermoset materials. *Molecules* **22**, 48 (2017).
29. F. Seniha Güner, Y. Yağcı and A. Tuncer Erciyes, Polymers from triglyceride oils. *Progress in Polymer Science* **31**, 633 (2006).
30. J.R. Kim, S. Sharma, The development and comparison of bio-thermoset plastics from epoxidized plant oils. *Industrial Crops and Products* **36**, 485 (2012).
31. P.Y. Kuo, M. Sain and N. Yan, Synthesis and characterization of an extractive-based bio-epoxy resin from beetle infested Pinus contorta bark. *Green Chemistry* **16**, 3483 (2014).
32. P.Y. Kuo, L.D. Barros, M. Sain, J.S. Y. Tjong and N. Yan, Effects of reaction parameters on the glycidyl etherification of bark extractives during bioepoxy resin synthesis. *ACS Sustainable Chemistry & Engineering* **4**, 1016 (2016).
33. C. Aouf, S. Benyahya, A. Esnouf, S. Caillol, B. Boutevin and H. Fulcrand, Tara tannins as phenolic precursors of thermosetting epoxy resins. *European Polymer Journal* **55**, 186 (2014).
34. Y. Celikbag, T.J. Robinson, B.K. Via, S. Adhikari and M.L. Auad, Pyrolysis oil substituted epoxy resin: Improved ratio optimization and crosslinking efficiency. *Journal of Applied Polymer Science* **132**, 9 (2015).
35. Y. Celikbag, S. Meadows, M. Barde, S. Adhikari, G. Buschle-Diller, M.L. Auad and B.K. Via, Synthesis and characterization of bio-oil-based self-curing epoxy resin. *Industrial & Engineering Chemistry Research* **56**, 9389 (2017).
36. B. Sibaja, C.P. Matheus, R.B. Mendez, J.R. Vega-Baudrit and M.L. Auad, Synthesis and characterization of interpenetrating polymer networks (IPNs) from acrylated soybean oil & α-resorcylic acid: Part 1: Kinetics of network formation. *Journal of Renewable Materials* **5**, 231 (2017).
37. B. Sibaja, C.P. Matheus, R.B. Mendez, R. Farag, J.R.V. Baudrit and M.L. Auad, Synthesis and characterization of interpenetrating polymer networks (IPNs) from acrylated soybean oil & α-resorcylic acid: Part 2: Thermo-mechanical properties and linear fracture mechanics. *Journal of Renewable Materials* **5**, 241 (2017).
38. S. Khadem and R.J. Marles, Monocyclic phenolic acids; hydroxy- and polyhydroxybenzoic acids: Occurrence and recent bioactivity studies. *Molecules* **15**, 7985 (2010).
39. R. Shakya, J. Whelen, S. Adhikari, R. Mahadevan and S. Neupane, Effect of temperature and Na_2CO_3 catalyst on hydrothermal liquefaction of algae. *Algal Research* **12**, 80 (2015).
40. H.X. Ben and A.J. Ragauskas, NMR characterization of pyrolysis oils from kraft lignin. *Energy Fuels* **25**, 2322 (2011).
41. G. Zhang, W. Choi, A low-cost sensitizer based on a phenolic resin for charge-transfer type photocatalysts working under visible light. *Chemical Communications* **48**, 10621 (2012).
42. C. Aouf, C. Le Guerneve, S. Caillol and H. Fulcrand, Study of the O-glycidylation of natural phenolic compounds: The relationship between the phenolic structure and the reaction mechanism. *Tetrahedron* **69**, 1345 (2013).
43. I.E. Dell'Erba and R.J.J. Williams, Homopolymerization of epoxy monomers initiated by 4-(dimethylamino)pyridine. *Polymer Engineering & Science* **46**, 351 (2006).
44. L.H. Sperling, *Introduction to Physical Polymer Science,* John Wiley & Sons, Inc, New Jersey, *355-365* (2006).
45. I. Poljansek and M. Krajnc, Characterization of phenol-formaldehyde prepolymer resins by in line FT-IR spectroscopy. *ACTA Chimica Slovenica* **52**, 238 (2005).

